Preparation of Layered $Li[Ni_{1/2}Mn_{1/2}]O_2$ by Ultrasonic Spray Pyrolysis Method

S. H. Park, S. K. Kang,[†] Y. C. Kang,[††] Y. S. Lee,[†††] and Y. K. Sun*
Department of Chemical Engineering, Hanyang University, Seoul 133-791, Korea
[†]*Division of Materials Science and Engineering, Hanyang University, Seoul 133-791, Korea*
[††]*Advanced Materials Division, Korea Research Institute of Chemical Technology, Daejon, 305-600, Korea*
[†††]*High-Tech Research Center, Kanagawa University, 3-27-1 Rokkakubashi, Yokohama 221-8686*

(Received February 6, 2003; CL-030112)

$Li[Ni_{1/2}Mn_{1/2}]O_2$ material was synthesized by ultrasonic spray pyrolysis method. $Li[Ni_{1/2}Mn_{1/2}]O_2$ was characterized by means of X-ray diffraction, charge/discharge cycling, and cyclic voltammetry. The discharge capacities of $Li/Li[Ni_{1/2}Mn_{1/2}]O_2$ cell at 30 and 55 °C slowly decreased with cycling and remained at 166 and 175 mAh/g after 50 cycles, which are 99 and 94% of initial capacities, respectively. The cyclic voltammogram studies of the $Li[Ni_{1/2}Mn_{1/2}]O_2$ electrode showed only one redox peak. This phenomenon might be related to the initial activation process and/or stabilization of $Li[Ni_{1/2}Mn_{1/2}]O_2$ electrode.

The layered lithium transition metal oxides $LiMO_2$ (M = Co, Ni, Mn) with a hexagonal α-$NaFeO_2$ structure have been expanded in the last a few years in the application as a cathode material for the lithium secondary batteries. $LiCoO_2$ has been commercialized, however, it has still some limits because of its high cost, moderate, and toxicity. $LiNiO_2$ and $LiMnO_2$ also have been extensively studied as possible alternatives to $LiCoO_2$. Although there have been much progress in optimizing the two materials, these still have some problems for the practical applications. $LiNiO_2$ is very difficult to use as a stoichiometric form, which needs very careful control in synthetic process and delithiated Li_xNiO_2 is easily decomposed exothermally at around 200 °C.[1–3] Also, $LiMnO_2$ form is not thermodynamically stable as the layered structure, especially orthorhombic phase of $LiMnO_2$.[4–6]

Recently, a concept of a one-to-one solid solution with atomic scale of $LiNiO_2$ and $LiMnO_2$, i.e., $Li[Ni_{1/2}Mn_{1/2}]O_2$, was reported by Ohzuku et al.[7] $Li/Li[Ni_{1/2}Mn_{1/2}]O_2$ cell delivered a reversible capacity of 150 mAh/g in the voltage range of 3.0 to 4.3 V with no indication of transformation to spinel phase during electrochemical cycling. Yoon et al. reported that Ni^{2+} and Mn^{4+} coexist in the layered $Li[Ni_{1/2}Mn_{1/2}]O_2$ material and Ni^{2+} ion is oxidized to Ni^{4+}, while Mn^{4+} ions remain mostly unchanged as Li is deintercalated from the material.[8] The stable cycling behavior of the $Li[Ni_{1/2}Mn_{1/2}]O_2$ material might be attributed to the stable tetravalent oxidation state of Mn ions during electrochemical cycling.

Considerable improvements of high performance cathode materials have been made by using solution method such as sol-gel method, coprecipiatation method, and spray pyrolysis method.[7–12] Among the solution methods, spray pyrolysis is an effective production technique leading to a good stoichiometric control, homogeneous powder, short production time, and one-step method. Recently, Taniguchi et al. reported that spherical spinel $LiMn_2O_4$ powder could be synthesized using spray pyrolysis method by varying gas flow rates and temperature profiles in the reactor.[12] In this study, we report on the synthesis and electrochemical characteristics of $Li[Ni_{1/2}Mn_{1/2}]O_2$ powder synthesized by ultrasonic spray pyrolysis method.

Layered $Li[Ni_{1/2}Mn_{1/2}]O_2$ powder was prepared as follows: $[Ni_{1/2}Mn_{1/2}]O_y$ precursor was first synthesized using a spray pyrolysis method. Nickel nitrate hexahydrate ($Ni(NO_3)\cdot 6H_2O$) and manganese nitrate hydrate ($Mn(NO_3)_2\cdot 4H_2O$) salts were used as starting materials for the synthesis of $[Ni_{1/2}Mn_{1/2}]O_y$ powder. Stoichiometric amounts of Ni and Mn nitrate salts (Ni/Mn = 1.0) were dissolved in distilled water. The dissolved solution was added into a continuously agitated aqueous citric acid solution. Citric acid was used as a polymeric agent for the reaction. The molar concentration of citric acid was fixed in 0.2 M. The starting solution was atomized using an ultrasonic nebulizer with a resonant frequency of 1.7 MHz. The aerosol stream was introduced into the vertical quartz reactor heated at 500 °C. The inner diameter and length of the quartz reactor are 50 and 1200 mm, respectively. The flow rate of air used as a carrier gas was 10 L/min. The prepared powders were mixed with an excess amount of $LiOH\cdot H_2O$. A small amount of lithium (Li/(Ni+Mn) = 1.05) was added to compensate for lithium evaporation during the calcination process. After the mixture was gently ground, these were heated at 900 °C 20 h after 500 °C 5 h in a box furnace with a heating rate of 1 °C/min.

The powder X-ray diffraction (XRD) using Cu Kα radiation was employed to identify the crystalline phase of the synthesized materials. The particle morphology of powder was observed using a scanning electron microscope (SEM). The electrochemical tests were performed using CR2032 coin-type cells. The cells were assembled as detailed elsewhere.[10] The charge and discharge cycling was performed at a current density of 0.2 mA/cm^2 (20 mA/g) with a cutoff voltage of 2.8-4.4 V at 30 °C and 55 °C.

Figure 1 shows X-ray diffraction (XRD) pattern of the $Li[Ni_{1/2}Mn_{1/2}]O_2$ powder with Miller indices indicated. All peaks can be indexed based on a hexagonal α-$NaFeO_2$ structure with a space group of $R\bar{3}m$. The XRD pattern of this material shows a single phase of layered structure and the peaks are quite narrow, indicating good crystallinity of the powder structure. This may be ascribed to the fact that the material derived from precursor is of atomic scale and homogeneously mixed with each other, and thus high sinterability. The pattern also shows a large inte-

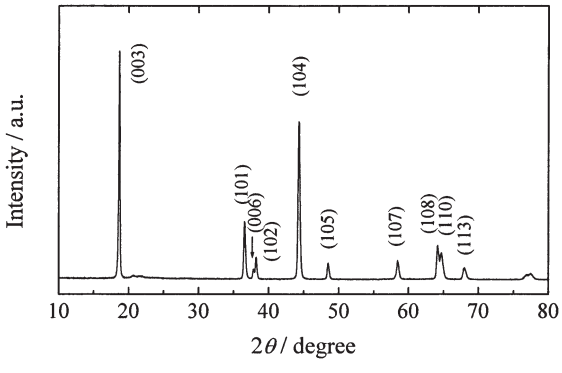

Figure 1. X-ray diffraction (XRD) pattern of $Li[Ni_{1/2}Mn_{1/2}]O_2$ powder.

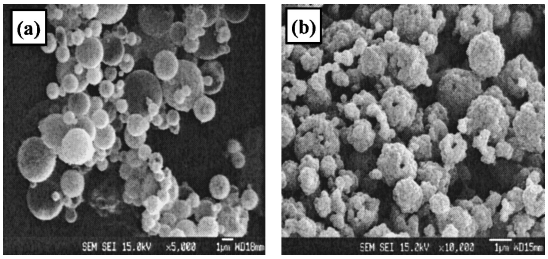

Figure 2. SEM images of (a) $[Ni_{1/2}Mn_{1/2}]O_y$, (b) $Li[Ni_{1/2}Mn_{1/2}]O_2$.

grated peak ratio (003) to (104) of 1.45 and a clear split of the (108) and (110) peaks, indicating less disorder in the host structure. The lattice constants of $Li[Ni_{1/2}Mn_{1/2}]O_2$ are determined to be $a = 2.880$ Å and $c = 14.276$ Å, which calculated by Rietveld refinement from the XRD data. This material shows a small difference between two patterns and R_{wp} of 10.08% strongly suggests a successful refinement between calculated and experimental patterns.[13] Therefore, it could be considered that $Li[Ni_{1/2}Mn_{1/2}]O_2$ material in this study has the $O3$ hexagonal structure with a space group of $R\bar{3}m$ (No. 166). Furthermore, we found that it is composed of lots of spherical secondary particles with 3-4 μm in diameter. The secondary particles, in turn, consist of spherical primary particles with approximately 200 nm as shown in Figure 2.

Figure 3 shows the charge/discharge curves and specific discharge capacities for the $Li/Li[Ni_{1/2}Mn_{1/2}]O_2$ cell as a function of cycle number between 2.8 and 4.4 V. The $Li/Li[Ni_{1/2}Mn_{1/2}]O_2$ cell (Figure 3a) shows very smooth and monotonous voltage profile as reported by other groups.[7,9] The $Li/Li[Ni_{1/2}Mn_{1/2}]O_2$ cell exhibits a small irreversible capacity (C_{disc}/C_{char}) of 14% in the first cycle, which is lower than that of lithium rich layered oxide ($Li[Li_{(1-2x)/3}Ni_xMn_{(2-x)/3}]O_2$).[10] It is noted that the charge/discharge curves showed no change even after 50 cycles, which means this $Li/Li[Ni_{1/2}Mn_{1/2}]O_2$ cell did not shown to the structural degradation during cycling. Figure 3b shows the specific discharge capacity vs number of cycle for the $Li/Li[Ni_{1/2}Mn_{1/2}]O_2$ cell at 30 and 55 °C at a constant current density 0.2 mA/cm^2 (1/8C). $Li/Li[Ni_{1/2}Mn_{1/2}]O_2$ cell delivers an initial discharge capacities of 167 and 187 mAh/g at 30 and 55 °C, respectively. The discharge capacities at 30 and 55 °C slowly decrease with cycling and remained at 166 and 175 mAh/g after 50 cycles, which are 99 and 94% of initial capacities, respectively. Although not presented

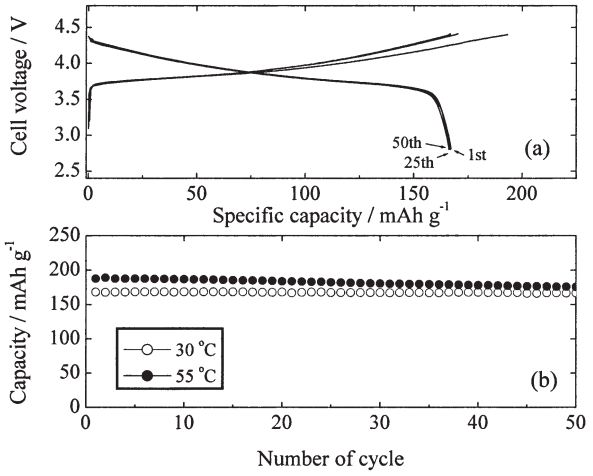

Figure 3. (a) Charge/discharge curves at 30 °C, (b) discharge capacity for $Li/Li[Ni_{1/2}Mn_{1/2}]O_2$ cells at various temperatures.

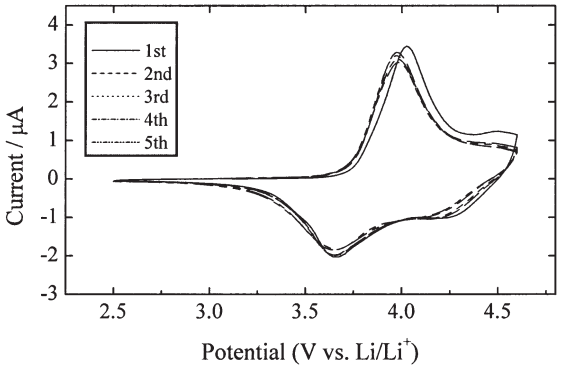

Figure 4. Cyclic voltamogram of $Li[Ni_{1/2}Mn_{1/2}]O_2$ between 2.5 and 4.6 V at a scan rate of 100 μVs^{-1}.

in this text, specific discharge capacity vs. number of cycle measurements for $Li/Li[Ni_{1/2}Mn_{1/2}]O_2$ cells cycled in various voltage ranges were also performed. The discharge capacities increase linearly with the increase of the upper cutoff voltage limit. In the voltage range of 2.8–4.3 V, 2.8–4.4 V, and 2.8–4.5 V, the discharge capacities of $Li[Ni_{1/2}Mn_{1/2}]O_2$ electrode were 155, 167, and 178 mAh/g, respectively, and these cells showed still excellent cycleabilities until 60 cycles.

Figure 4 shows the cyclic voltammogram of the first five cycles of the $Li[Ni_{1/2}Mn_{1/2}]O_2$ electrode between 2.5 and 4.6 V. It could be observed that, similarly to charge/discharge curve, the profile of the first anodic peaks is slightly different from the subsequent ones. The first anodic scan has two oxidation peaks, a major peak centered at 4.02 V and a minor one at 4.5 V, corresponding to irreversible capacity observed in the first charge profile. The peak 4.02 V in the first anodic scan is shifted by 0.05 V to lower voltage and remains unchanged for the subsequent cycles. The reduction peak observed at 4.3 V during the first cycle disappears after 3 cycles and there is the only one major peak centered at 3.97 V in cathodic process. This phenomenon might relate to the initial activation process and/or stabilization of the $Li[Ni_{1/2}Mn_{1/2}]O_2$ electrode. This implies that structural degradation does not expected during the lithium extraction/insertion process of the $Li[Ni_{1/2}Mn_{1/2}]O_2$ electrode unlike that of $LiNiO_2$.[1,14] The cyclic voltammogram study of the $Li[Ni_{1/2}Mn_{1/2}]O_2$ electrode showed only one redox peak, indicating that structural phase transitions did not occur during electrochemical cycling.

This work was supported by KOSEF through the Research Center for Energy Conversion and Storage.

References

1 J. R. Dahn, E. W. Fuller, M. Obrovac, and U. von Sacken, *Solid State Ionics*, **69**, 265 (1994).
2 H. Arai and Y. Sakurai, *J. Power Sources*, **81-82**, 401 (1999).
3 T. Ohzuku, A. Ueda, and M. Kouguchi, *J. Electrochem. Soc.*, **142**, 4033 (1995).
4 B. Ammundsen and J. Paulsen, *Adv. Mater.*, **13**, 943 (2001).
5 G. Vitins and K. West, *J. Electrochem. Soc.*, **144**, 2587 (1997).
6 Y.-I. Jang, B. Huang, Y.-M. Chiang, and D. R. Sadoway, *Electrochem. Solid-State Lett.*, **1**, 13 (1998).
7 T. Ohzuku and Y. Makimura, *Chem. Lett.*, **2001**, 744.
8 W.-S. Yoon, Y. Paik, X.-Q. Yang, M. Balasubramanian, J. McBreen, and C. P. Grey, *Electrochem. Solid-State Lett.*, **5**, A263 (2002).
9 Z. Lu, D. D. MacNeil, and J. R. Dahn, *Electrochem. Solid-State Lett.*, **4**, A200 (2001).
10 S.-S. Shin, Y.-K. Sun, and K. Amine, *J. Power Sources*, **112**, 634 (2002).
11 T. Ogihara, N. Ogata, K. Katayama, Y. Azuma, and N. Mizutani, *Electrochemistry*, **68**, 162 (2000).
12 I. Taniguchi, C. K. Lim, D. Song, and M. Wakihara, *Solid Stat Ionics*, **146**, 239 (2002).
13 F. Izumi, *Nippon Kessho Gakkaishi*, **27**, 23 (1985).
14 G. Gutta, A. manthiram, and J. B. Goodenough, *J. Sold State Chem.*, **96**, 123 (1992).

Published on the web (Advance View) April 16, 2003; DOI 10.1246/cl.2003.446